Study of the static and dynamic behavior of PU foams: from the sample to the automotive seat.

Corentin Blanchard[1,2], Thomas Weisser[2], Romain Barbeau[1],
Anne-Isabelle Mallet-Da Costa[1], Evelyne Aubry[2]
[1]Faurecia Automotive Seating, CS 10001, 91152 Etampes, France
[2]IRIMAS, Université de Haute-Alsace, 2 rue des Frères Lumière, 68093 Mulhouse Cedex
corentin.blanchard@uha.fr

Abstract

This study concerns the vibrational comfort of automotive seats. It is commonly characterized by the seat transmissibility, obtained by computing the ratio of the acceleration at the seat surface to the one at the seat base. This curve, observed in the frequency domain, depicts the seat performance in terms of vibrations filtration. The transmissibility is computed on a loaded structure, which means that an initial compression is present. Since the complete seat is a complex system, the first part of the paper presents static and dynamic experiments and simulations on a foam sample. The experiments are then reproduced using a finite element model. In the case of the static compression tests, the stress-strain curve is chosen as validation criterion. The simulation shows that for strains lower than 75%, the model is accurate. In the case of the dynamic experiment, the measured and simulated transmissibilities are compared. While the resonance and cut-off frequencies are close to the experimental results, the gain at the resonance is overestimated. The second section presents static and dynamic measurements performed on a seat cushion loaded by a rigid mass. The results show that the trim has an impact on the measured displacements and pressure distributions. In dynamics, it also has an impact on the resonance peak of the transmissibility. Finally, the simulation process proposed to validate the complete seat model is presented.

1 Introduction

The automotive sector faces new evolutions caused by the arrival of new features such as partial or full automated driving. These evolutions allow to have new reflections on the various postures that could be adopted by the occupants. This leads car manufacturers and suppliers to consider different seating positions. The driving position, where the occupant sits while holding the steering wheel, remains the most common. However, other positions are studied, such as the working position, where the occupant does not touch the steering wheel while the backrest is slightly reclined, or the relax position, where it is almost lying on the seat, are some examples.

Given these new reflections, the seat design remains constrained, either externally (by regulations or norms) or internally (depending on the features that need to be implemented). The present study focuses on the vibrational comfort, which is an internal constraint. The seat vibrational comfort is observed by measuring its transmissibility. It is obtained by computing the ratio of the transmissibility at the seat surface to the one at the seat base. The measurement has to be performed when an occupant sits on the seat. Three different classes of occupants can be considered : rigid masses, manikins and human subjects.

It is important to see this measurement as two separate steps: first, the occupant is placed on the seat. At the end of this step, the seat is deformed and a steady state is reached, corresponding to the equilibrium between the weight of the occupant and the reaction forces in the seat. The second step is the dynamic measurement itself, which consists in measuring the acceleration at the surface and at the base of the seat to derive the corresponding transmissibility.

The goal of this study is to perform such a process using a finite element model, which raises questions about the foam modeling. Indeed, transmissibility measurements using a rigid mass performed by Barbeau [6] show that the foam has a strong influence on the transmissibility. The polyurethane foam belongs to the viscoelastic materials, and its static and dynamic behaviors are non-linear. The validation must therefore be conducted at each step. To validate the results from the static step, it is possible to use different kind of measurements. For

instance, Zhang [4] uses force-displacement curves, Siefert et al. [3] compare the final displacement on the cushion and backrest, and Verver [9] works with pressure maps measurements. Regarding the dynamic step, the transmissibility is the criteria chosen in the articles from Zhang and Siefert et al.

Several authors have chosen to conduct deeper investigation of the foam behavior, and have therefore worked on foam samples. Krishan [7] and Verver [9] use tabulated stress-strain curves to model foam samples and use the data to conduct parametric studies. Siefert et al. [3] and Grujicic [10] have used analytical models and implemented them in complete seat models. Martinez-Agirre [2] or Lee and Kim [5] also propose dynamic models which take the initial deformation as an additional parameter, but this concerns other viscoelastic materials (rubber and thin films).

The goal of this study is to investigate the possible bridges between the material characterization at the sample scale and the experimental measurements at the seat scale. The first section regards the study of foam samples. It will be split into two steps: static and dynamic characterization. For each step, experimental validation is presented. The second section regards the experimental measurements conducted on the seat and introduces the simulation process to be used.

2 Analyses on a foam sample

The complete seat is considered as a complex system due to the high number of subcomponents involved. To properly simulate its global behavior, it is important to have accurate models for each of its subcomponents. This first section aims at studying the static and dynamic behaviors of the polyurethane foam used for the seat cushion and backrest. To do so, the analyses are carried on academic foam samples. The goal is to extract values that can be used as input data for static and dynamic simulations using a finite element model.

2.1 Static analysis

2.1.1 Measurements

The static characterization of the foam sample is done by measuring its stress-strain curves using an Instron 33R4204 machine following the protocol described in the ISO 3386-1 norm [11].

Three samples were used, each of them measuring $95mm \times 95mm \times 40mm$ and weighting $14g$. The choice of their size was dictated by the fact that they were cut out of the seat cushion and by the length/height ratio specified in the norm (equal or greater than 2). Five compression-decompression cycles are performed at $100mm/min$ up to 80% of deformation. The results are presented in figure 1.

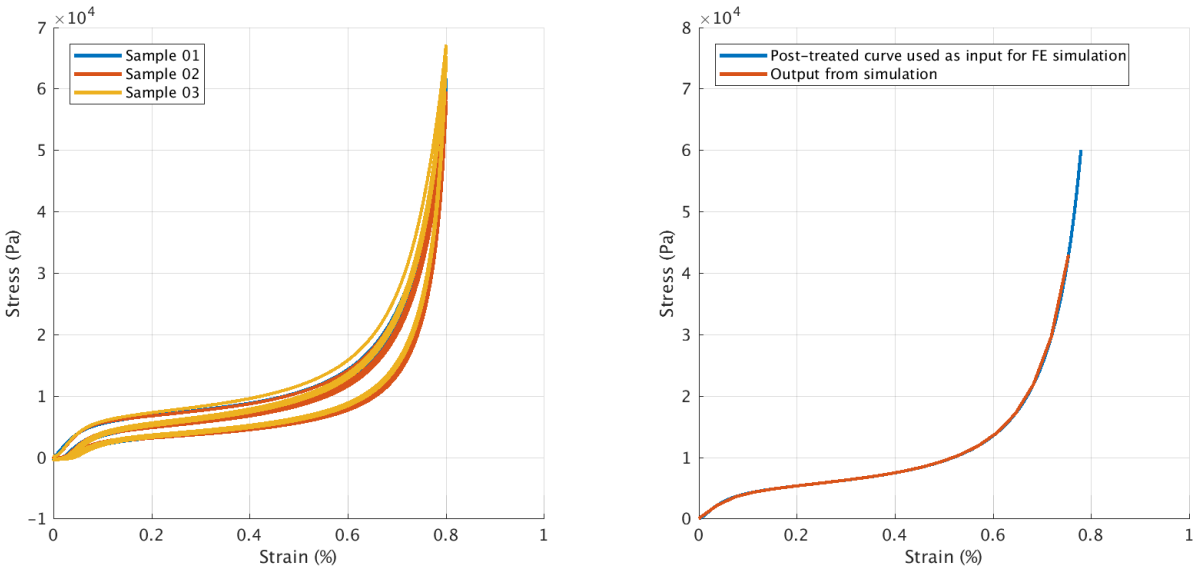

Figure 1: Left: Raw stress-strain curves measured on three foam samples. Right: Post-processed curve used as input for the finite element simulation (blue) and simulation result (red).

Although the curves associated to the first cycle are different depending on the sample, it is possible to observe the typical behavior of the foam in the three cases. First, a linear-elastic behavior for strains less than 5%, then a plateau region from 5% to 60%, and finally a densification region above 60%. It is also possible to see that, although the loading curves are different with regards to the cycle, the unloading curve always follows the same path. Finally, after the first cycle, the stress-strain curves are shifted, which is called the Mullins effect [1]. Each curve represents the static behavior of the foam sample and can be used as input data for the finite element model which is presented below.

2.1.2 Finite Element simulation

The use of the tabulated stress-strain curve for the foam static behavior is validated by conducting a simulation that reproduces the test presented above. The model consists in a foam sample made of 3D elements (ca. 4000 nodes and 3000 elements). The associated material model uses a stress-strain curve as input [8]. The last cycle of the experimental curve is extracted and only the compression part is used. An offset is applied to remove the Mullins effect from the curve and to make it start at the origin, see figure 1.

The compression is performed by prescribing a displacement at the top surface of the foam sample. The top surface is compressed at the same speed than the experiment up to 75%. The goal is to ensure that the stress-stain curve is accurately interpreted by the solver. The results are presented in figure 1. The comparison of the experimental and simulated stress-strain curves shows that the simulated curve follows the same path as the experimental curve.

2.2 Dynamic analysis

The static characterization of the foam is followed by its dynamic characterization. In this study, the transmissibility curve of a foam sample is presented.

2.2.1 Measurements

The dynamic characterization of the foam sample, performed by Barbeau [6], is made using its transmissibility curve. The sample is placed on a flat surface and is compressed by adding additionnal masses until reaching 30% of compression. This value is chosen based on Faurecia's know-how and corresponds to a commonly measured value when using an automotive seat. Then, a swept sine from 3 to $19Hz$ with a displacement amplitude of $\pm 0.5mm$ is applied at the base of the sample using a vibration shaker. The acceleration at the base $a_{base}(\omega)$ and at the surface $a_{top}(\omega)$ are measured. The ratio $T(\omega) = a_{top}(\omega)/a_{base}(\omega)$ is then computed and represented in figure 2.

Three parameters can be extracted from the transmissibility curve:

- The resonance frequency f_r: the frequency at which the transmissibility reaches its highest value,
- The gain at the resonance G_r: the value of the transmissibility at the resonance frequency,
- The cut-off frequency f_c: the frequency after which the transmissibility is lower than 1, thus characterizing the beginning of the filtration zone.

For the considered foam sample, the resonance frequency is $f_r = 5.81Hz$, the gain at the resonance is $G_r = 5.05$ and the cut-off frequency is $f_c = 8.95Hz$ (see table 1). The goal is then to compare these experimental results with the simulated transmissibility.

2.2.2 Finite Element simulation

Similarly to the static analysis, a finite element model of this experiment is built. The model consists in two parts, representing the foam sample and the rigid mass respectively. The mass density of the rigid part is chosen so that the part has the same mass as the experimental masses used to compress the foam at 30%.

The simulation process is divided into two steps. The first step is a simulation of the sinking of the mass. In that case, the material model used for the foam part takes the stress-strain curve as input. The gravity is applied to the model and the vertical displacement of the rigid mass is monitored. At the end of the simulation, the

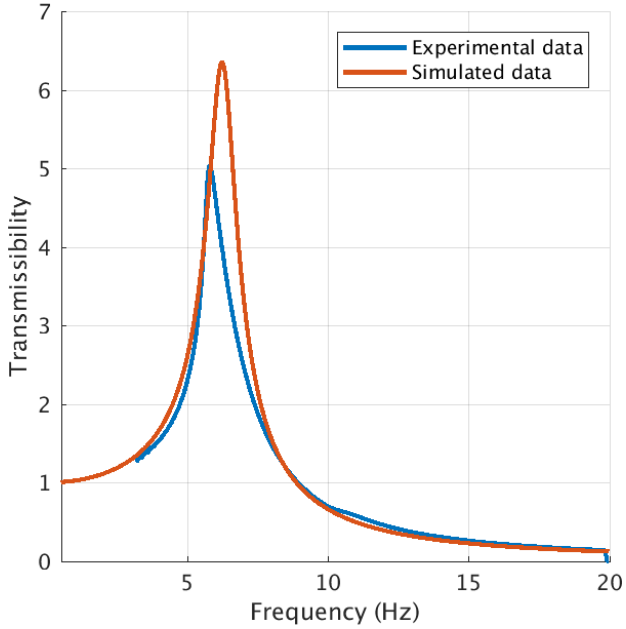

Figure 2: Experimental transmissibility curve (blue) and simulated curve with an equivalent elasticity modulus (red).

sample is compressed at 30%. The final state of the model (i.e. the nodal coordinates and the material stresses tensors) is exported and used as input for the dynamic simulation.

The second step is the dynamic simulation. In that case, the material model used for the foam needs to be changed. Indeed, when considering initial stresses with a material defined by its stress-strain curve, the solver computes an equivalent linear elasticity modulus taken as the tangent of the curve. Since the sample is compressed at 30%, this corresponds to the plateau zone. In that case, using the tangent modulus would result in a non-physical behavior.

To counter this problem, the transmissibility curve is approximated using the transmissibility of a 1-DOF mass-spring-damper system. Indeed, it is assumed that the excitation amplitude applied for the transmissibility measurement is low enough to excite the linear behavior of the material. For such a system, the transmissibility is defined as:

$$T(\omega) = \frac{k + jc\omega}{-m\omega^2 + jc\omega + k}, \tag{1}$$

where m, k and c are the mass, stiffness and damping coefficients of the equivalent model. Since m is known, the stiffness can be found using $k \approx m\,(2\pi f_r)^2$. The damping coefficient c is found using the graphical method of the $-3dB$ bandwidth. Here, $m = 8.3kg$ and the identified values are $k = 11000Nm^{-1}$ and $c = 47.1Nm^{-1}s$. The elasticity modulus is then found using the fact that $k = \frac{ES}{l}$, with S the sample top surface area and l the sample height. The associated modulus is then $E = 44000Pa$. This value is used as input for the linear-elastic material model used for the foam.

The transmissibility is computed using the modal superposition method. A modal damping of ζ defined as $\zeta = \frac{c}{2\sqrt{km}} = 0.08$ is used. The results are presented in figure 2. The comparison of both curves shows that the resonance frequency f_r and the cut-off frequency f_c are well caught. However, the gain at the resonance is overestimated. Table 1 summarizes the parameters derived from both transmissibility curves. This comparison shows the limitations of the asumption of linear behavior. Another way to see this is to notice that the resonance peak is inclined towards the left, indicating a softening behavior which is not captured with a linear 1-DOF hypothesis.

This concludes the analyses on the foam sample. The goal is then to apply this methodology to the automotive seat. The following section presents the different measurements performed on the automotive seat as well as the simulation process which is considered.

	Experimental	Simulated	Relative difference (ref. experimental)
f_r (Hz)	5.81	6.22	7%
G_r (.)	5.05	6.35	25.7%
f_c (Hz)	8.95	8.88	−0.8%

Table 1: Comparison of the parameters derived from the experimental and simulated transmissibilities.

3 Analyses on the automotive seat

As in the previous section, the analysis on the complete seat is divided into two steps: the static analysis, where the deformation of the seat under the load due to an occupant is studied, and then the dynamic analysis where the vibrational behavior of the seat is studied.

The seat chosen for the present study is a serial production seat used from a C-segment production car. It can be divided into 4 main subcomponents: a frame made of metal parts that corresponds to the main structure of the seat; two suspension mats, that are an assembly of metal wires and plastic parts, which are used for static comfort; the foam pads and the seat cover. The complete seat is represented in figure 3.

Figure 3: Exploded view of the complete seat finite element model.

3.1 Static analysis

As said above, before studying the seat vibrational behavior, a static analysis has to be performed. Its goal is to obtain the deformation of the seat under the load due to a given occupant. Three occupants can be distinguished: rigid masses, dummies or human subjects. Here, a rigid mass has been chosen to ensure the repeatability of the experimental results. The one used for the present stydy is called a lead buttock. It is made of a part that has the shape of the human thighs and buttocks connected to an arm. The whole structure is rigid and connected to the jig with a revolute joint.

To compare experimental and simulated data, a common point is needed. This point is called the Hip point (H-point) and corresponds to the pivot between the torso and the upper legs for a 50th percentile male occupant. During the design process, the H-point position is defined and the seat is defined using it as a reference. This point will be used to ensure that the rigid mass is accurately placed on the seat.

3.1.1 Measurements

The first measurement is the sinking of the lead buttock into the seat. To do so, the H-point of the lead buttock has to be placed at the H-point of the seat. Due to the geometry of the arm, this is not possible when the backrest is mounted. To ensure that both H-points are coincident, the backrest is therefore removed. Finally, the measurements are made according to two setups: first, when the seat is untrimmed (i.e. with no fabric cover on the foam cushion) and with the fabric cover.

The lead buttock is first placed so that its H-point matches seat one. The angle of the arm has to be nil to ensure that the angle of the lead buttock is 18°. This value corresponds to the femur angle of a seated human subject (15°) and a 3° tilt applied to compensate for thigh flexibility since the lead buttock is rigid. The sinking of the lead buttock is computed by measuring the distance between a point on the suspension mat with and without the occupant. This point is chosen in order to have the same X-coordinate than the H-point.

Values of the H-point as well as the sinking for each setup (untrimmed and trimmed seat) are presented in table 2, along with the nominal values taken as reference. The results show that the sinking of the lead buttock is lower when the seat is untrimmed. This shows that when the seat is untrimmed, the lead buttock sinks mainly in the foam (hence the lower value of the Z-coordinate), whereas when the seat is trimmed, the deformation is transferred to the suspension mat (hence the higher mat deformation).

	Nominal values (CAD)	**Trimmed seat**	**Untrimmed seat**
H-point X-coordinate (*mm*)	1256.6	1259.8	1259.4
H-point Z-coordinate (*mm*)	315	297.4	293
Mat deformation	NA	11.3	10.9

Table 2: Comparison between theoretical and measured values for the H-point and the mat deformation according to the seat setup.

The second static measurement available is the pressure map. Using a pressure sensor mat, it is possible to obtain the pressure distribution over the contact surface. The measurements have been performed on the trimmed and untrimmed seat following an internal Faurecia standard [13] with the lead buttock. The results are presented in figure 4. Both measurements present the same pattern, with a main contact surface reprensenting the bottom of the thighs, and three additional surfaces associated to the contact between the lead buttock and the seat bolsters.

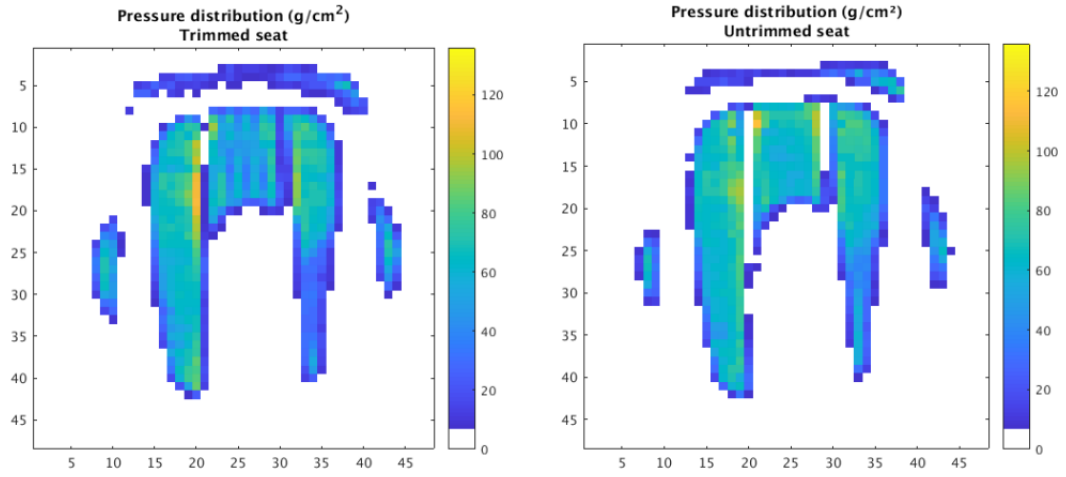

Figure 4: Pressure maps obtained depending on the seat setup.

Four parameters can be extracted from these measurements: the contact surface area, and the minimum, average and peak pressure. The values obtained for the two measurements are presented in table 3. Regarding the contact surface, the area measured for the untrimmed seat is 3.5% lower than the one obtained for the trimmed seat. Regarding the pressure, while the minimum value remains the same (i.e. the lowest value that can be measured by the sensors), the average and peak pressures are 13.2% and 2.5% higher respectively. This shows the impact of the trim, which helps to distribute the applied pressure over a larger area, thus resulting in

a lower average pressure.

	Trimmed seat	Untrimmed seat	Relative difference
Contact surface area (cm^2)	1033.87	956.45	-7.5%
Minimum pressure ($g.cm^{-2}$)	6.82	6.80	-0.3%
Average pressure ($g.cm^{-2}$)	42.94	48.62	13.2%
Maximum pressure ($g.cm^{-2}$)	111.93	114.7	2.5%

Table 3: Comparison between theoretical and measured values for the H-point and the mat deformation according to the seat setup.

It is interesing to see that the maximum pressure is $114.7 g.cm^{-2}$. When this value is multiplied by the gravity acceleration ($g = 9.81 ms^{-2}$), it is possible to obtain the maximum applied stress. Here, $\sigma_{max,exp} = 11.25 kPa$. This value is lower than the maximum stress obtained in the simulation ($\sigma_{max,sim} = 43 kPa$, see figure 1) and shows therefore that the tabulted curve can be used for simulations on the seat.

After the static characterization of the seat, the dynamic characterization is performed. Like the study on the foam sample, the transmissibility will be used.

3.2 Dynamic analysis on the seat cushion

3.2.1 Measurements

Following the static measurements on the seat cushion using the lead buttock, the dynamic analysis is performed. The seat and the lead buttock are kept in the same position as the static measurements and the transmissibility of the system is measured.

The experimental protocol is defined by an internal standard [12]. The excitation signal is a white noise with a bandwidth from 2 to $30 Hz$ and with an RMS value of $0.5 ms^{-2}$. The seat is first excited during $2 min$ until the steady state is considered as reached, and then the measurement is performed during $6 min$. Two accelerometers are placed on the test bench to measure the acceleration at the base $a_{base}(\omega)$ and at the lead buttock H-point $a_{H-point}(\omega)$. The transmissibility is then computed as $T(\omega) = a_{H-point}(\omega)/a_{base}(\omega)$. Once again, the measurements have been performed on the trimmed and untrimmed seat. In each case, the measurements have been done twice. The resulting curves are presented in figure 5 and the derived parameters are listed in table 4.

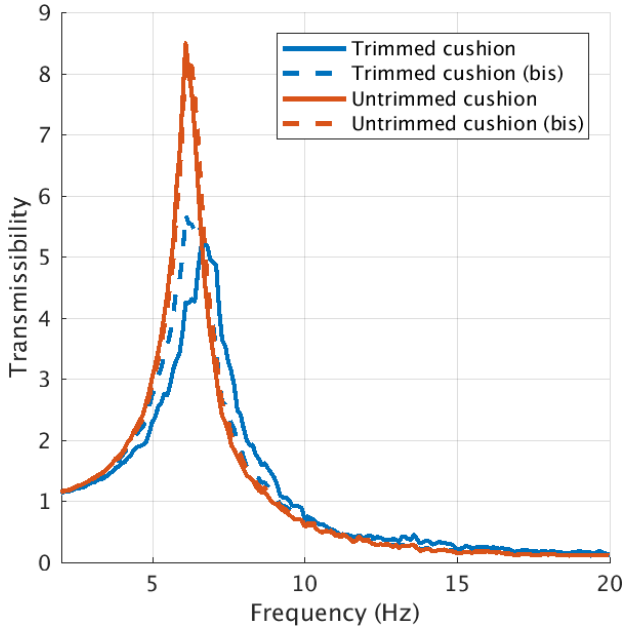

Figure 5: Transmissibilites obtained for the trimmed and untrimmed seat cushion with a lead buttock.

These measurements show the influence of the trim on the transmissibility curve. Indeed, when the seat cushion is trimmed, the gain at the resonance G_r decreases while the cut-off frequency f_c increases. The impact

	f_r (Hz)	G_r (.)	f_c (Hz)
Trimmed cushion	6.80	5.19	9.51
Trimmed cushion (bis)	6.10	5.69	9.15
Untrimmed cushion	6.10	8.50	8.90
Untrimmed cushion (bis)	6.10	8.28	9.08

Table 4: Values of the derived parameters depending on the seat setup.

of the trim on the resonance frequency f_r is harder to evaluate because of the strong difference between the two measurements for the trimmed cushion. When the seat is trimmed, damping is added and results in a lower but wider resonance peak.

3.3 Simulations

These experimental results have to be compared with numerical simulations to ensure that the modelling choices retained for the seat are valid. The simulation process is similar to the one applied to the foam sample.

The static analysis is performed by computing the sinking of the lead buttock on the seat cushion. The lead buttock is placed above the seat and the gravity is applied to the model. The material law used for the foam is the one from figure 1. The first goal of this simulation is to validate the model using experimental data: the location of the H-point, the arm angle, the mat deformation and the pressure maps are the four criteria that can be used. The comparison can be done with the results presented in tables 2 and 3 and in figure 4. The second goal of this simulation is to extract the final state of the model (deformed geometry and internal stresses).

This final state is then used as input for the dynamic simulation. Like the dynamic simulations done with the foam sample, a different material law than the one used for the static simulations needs to be used. The choice of the material model for the foam will be critical since the results of the dynamic simulations on the foam sample show that the use of an equivalent linear elasticity modulus overestimates the gain at the resonance. The results from this simulation have to be compared with values from figure 5 and 1.

4 Conclusions

In the first part of this study, the static and dynamic behaviors of foam samples are studied. The goal is to develop finite element models that match the physical behavior of the foam. The foam static behavior is obtained by performing compression-decompression tests. This allows to obtain the stress-strain curve of the material, which is then used for the finite element simulation. The results show that the model fits the experimental data up to 75% of deformation. The foam sample is then dynamically characterized by measuring its transmissibility. By assuming that the system behaves like a 1-DOF system, it is possible to extract linear-elastic equivalent parameters that will be used for the finite element simulation. The comparison shows that the resonance frequency and the cut-off frequency are well found, but the gain at the resonance is overestimated.

In the second part of this study, static and dynamic measurements performed on an automotive seat are performed. In statics, sinking and pressure distribution are performed when it is loaded with a rigid mass. When the seat is untrimmed, the rigid mat causes less suspension mat deformation and results in a higher average pressure on a smaller contact surface area, thus showing the role of the trim. In dynamics, transmissbilites of both setups are measured. The impact of the trim is confirmed since the resonance peak is lower and wider when the seat is trimmed.

While the use of a tabulated stress-strain curve allows to properly simulate the static behavior of the foam, it is shown that the modelling choices for its dynamic behavior could be improved. The asumption of a linear behavior of the elasticity modulus over the studied frequency range should then be rethought. A possible solution would be to use an enhanced model. The choice of such a model should be guided by additional measurements on the foam samples to characterize its material properties. This could also allow to study the influence of external factors such as the excitation frequency.

References

[1] L. Mullins, Effect of stretching on the properties of rubber, Rubber Chemistry and Technology, 21(2) (1948) 281–300.

[2] M. Martinez-Agirre, S. Illescas, M. J. Elejabarrieta, Characterisation and modelling of prestrained viscoelastic films, International Journal of Adhesion & Adhesives, 50 (2014) 183–190.

[3] A. Siefert, S. Pankoke, H.-P. Wölfel, Virtual optimisation of car passenger seats: Simulation of static and dynamic effects on drivers' seating comfort, International Journal of Industrial Ergonomics, 38 (2008) 410–424.

[4] X. Zhang, Y. Qiu, M. Griffin, Developing a simplified finite element model of a car seat with occupant for predicting vibration transmissibility in the vertical direction, Ergonomics, 58 (2015) 1–12.

[5] J.-H. Lee, K.-J. Kim Characterization of Complex Modulus of Viscoelastic Materials Subject to Static Compression, Mechanics of Time-Dependent Materials, 5 (2001) 255–271.

[6] R. Barbeau, Characterization and modeling of automotive seat dynamics: toward the robust optimization of vibrational comfort. Thèse, Université de Haute-Alsace, 2018.

[7] K. Krishan, Occupant-Seat Contact Pressure Characteristics of Polyurethane Foam Seats Using Explicit Finite-Element Analyses. Master's Thesis, Concordia University, 2017.

[8] LSTC, LS-DYNA Keyword User's Manual, Volumes I-III, Online, Accessed on Mai 28th 2019, Livermore, 2014.

[9] M. M. Verver, J. van Hoof, C. W. J. Oomens, J. S. H. M. Wismans, F. P. T. Baaijens, A finite element model of the human buttocks for prediction of seat pressure distributions, Computer Methods in Biomechanics and Biomedical Engineering, 7 (2004) 193–203.

[10] M. Grujicic, B. Pandurangan, G. Arakere, W. C. Bell, T. He, X.Xie, Seat-cushion and soft-tissue material modeling and a finite element investigation of the seating comfort for passenger-vehicle occupants, Materials and Design, 30 (2009) 42773–4285.

[11] International Organization for Standardization (ISO), ISO 3386-1 Determination of stress-strain characteristic in compression, Online, Accessed on Mai 29th 2019, 1998.

[12] GRP S RDT 1005, Evaluation de la réponse dynamique de l'assise d'un siège, Faurecia Standard, 2002.

[13] RBR I DSS 9450, Pressure mat Comfort Test Xsensor Procedure - Human Subject, Faurecia Standard, 2011.